DOI: https://doi.org/10.2138/am-2022-7990. http://www.minsocam.org/

Revision 2

Oxygen isotope heterogeneity of olivine crystals in orogenic peridotites from Songshugou, North Qinling Orogen: Petrogenesis and geodynamic implications

Hong Yu[1*], Hong-Fu Zhang[2,3], Haibo Zou[4], Ji-Feng Xu[1]

[1] State Key Laboratory of Geological Processes and Mineral Resources, and School of Earth Science and Resources, China University of Geosciences, Beijing 100083, China

[2] State Key Laboratory of Lithospheric Evolution, Institute of Geology and Geophysics, Chinese Academy of Sciences, Beijing 100029, China

[3] State Key Laboratory of Continental Dynamics, Department of Geology, Northwest University, Xi'an 710069, China

[4] Department of Geosciences, Auburn University, Auburn, AL 36849, USA

[*]corresponding author: Hong Yu, yuhong@cugb.edu.cn

Abstract

Olivine grains from Songshugou mylonitized peridotite massif record $\delta^{18}O$ both lower and higher than in pristine mantle samples in North Qinling Orogen, Central China. Olivines from dunites exhibit large variations in $\delta^{18}O$ (4.03-7.07‰), and some porphyroclasts display negative correlations between $\delta^{18}O$ and forsterite content (Fo; [100×Mg/(Mg+Fe^{2+})]). The porphyroclast cores have low $\delta^{18}O$ values, indicating that they formed in the oceanic lithospheric mantle prior to subduction. We attribute low $\delta^{18}O$ values to seawater-peridotite interaction under high temperature conditions. The porphyroclast rims and small olivines exhibit high $\delta^{18}O$ values. These features suggest that high-$\delta^{18}O$ olivines formed during mylonitization in the exhumation process. Olivines reacted with ^{18}O-rich melt/fluids released from subducted altered oceanic basalts and continental sediments at low temperature (<610-680 °C). The ^{18}O-rich melt/fluids selectively affected porphyroclast rims and small olivine grains. Unlike the olivines in the dunites, the olivines and orthopyroxenes in the harzburgites show limited variations in $\delta^{18}O$ (4.21-5.45‰ and 5.5-5.8‰, respectively), due to orthopyroxene exchange with melt/fluid at a slower rate than the coexisting olivine. The preservation of the low-$\delta^{18}O$ signature in olivines indicates a short residence time (<20 Ma) for subducting peridotites to mantle depths.

Keywords: Oxygen isotope heterogeneity; Olivine; Orthopyroxene; Songshugou peridotites; North Qinling Orogen

DOI: https://doi.org/10.2138/am-2022-7990. http://www.minsocam.org/

1. Introduction

The formation and evolution of the orogenic peridotites is an important topic in solid earth science. The oxygen isotopic compositions of minerals from orogenic peridotites can provide important geodynamic insights. Numerous investigations have established that continental crustal materials have been recycled into the mantle and interacted with peridotites through oceanic subduction to continental collision during the orogenic process (Barnicoat and Cartwright 1995; Zheng et al. 1998; Michael et al., 2000; Dijkstra et al., 2002; Song et al. 2006; Zou et al. 2017). The distinction between oxygen isotopic compositions of mantle versus crustal materials suits the system well to studies of magma source and evolution (Bindeman et al. 2008; Wang and Eiler 2008; Genske et al. 2013; Moore et al. 2016; Kim et al. 2021), metamorphism of crustal rocks (Barnicoat and Cartwright 1997; Zheng et al. 1998; Putlitz et al. 2000; Riches et al. 2016), as well as mantle metasomatism (Deines and Haggerty 2000; Widom and Farquhar 2003; Perkins et al. 2006; Guo et al. 2013; Liu et al. 2014; Hao et al. 2016; Marshall et al., 2017; Dallai et a., 2019). Pristine mantle peridotites generally have homogeneous oxygen isotope compositions of $\delta^{18}O=5.7\pm0.2‰$ (Mattey et al. 1994; Harmon and Hoefs 1995; Eiler et al. 1997). However, where orogenic peridotites have undergone subduction with crustal materials and experienced HP-UHP metamorphism, they may have oxygen isotopic compositions remarkably different from the normal mantle. During subduction, devolatilization of the hydrated oceanic crust and continental sediments releases substantial amounts of fluid with variable $\delta^{18}O$ compositions. The $\delta^{18}O$ values of orogenic peridotites increase through interaction with melt/fluid of high-^{18}O composition derived from sediments (Dobosi et al. 2003; Liu et al. 2015; Hu et al. 2019), low-T altered oceanic crust and carbonates (Gregory and Taylor 1981; Vroon et al. 2001; Carmody et al. 2013; Jakob et al. 2018), and decrease through meteoric/hydrothermal fluid and seawater interaction (Stakes and Taylor 1992; Putlitz et al. 2000; Rouméjon et al. 2018; Sharp et al. 2018; Radu et al. 2019; Zakharov and Bindeman 2019). Thus, oxygen isotopes can be applied to deciphering potential origin of the varied rocks found in orogenic belts, but little research has been conducted in the formation processes of orogenic peridotites.

The Songshugou mylonitized peridotite massif occur as several hundred blocks within amphibolites of the Qinling Group, North Qinling Orogen of Central China. The petrogenesis and tectonic implications of these peridotites is under debate. One model considers the Songshugou peridotites as fragments of oceanic lithosphere formed during the late Mesoproterozoic to early Neoproterozoic (Wang et al. 2005; Dong et al. 2008; Nie et al. 2017; Sun et al. 2019;). Some authors argue against this notion and regard the rock as a cumulate of ultramafic magma (Song et al. 1998), or a melt-rock reaction product associated with mantle plume activity (Su et al. 2005), or as melting residue in forearc mantle (Cao et al. 2016). Recent studies suggest that the Songshugou peridotites represent fragments of the Neoproterozoic oceanic lithospheric mantle which experienced subduction and exhumation together with the Qinling Group during the Paleozoic (Zhang et al. 2015; Yu et al. 2017, 2019; Rui et al. 2019). The process resulted in the alignment of elongated olivine (Ol) grains from initially coarse-granular via porphyroclastic to finegranular texture. The high amphibole content, relatively low forsterite content (Fo; [100×Mg/(Mg+Fe^{2+})]), together with high Al_2O_3, and CaO contents and the abnormally low total PGE abundance in the mylonitized fine-grained dunites suggest the ingress of melt/fluid during subduction and exhumation (Yu et al. 2017). Studies of the O and Lu-Hf isotope systematics of zircon from Songshugou amphibolites which experienced subduction along with the peridotites also indicate the ingress of melt and fluid from altered oceanic basalts and continental sediments (Yu et al. 2016). Oxygen isotopes in major minerals which interacted with melts/fluids can help with understanding geochemical processes involving metamorphism at mantle and crust depths, and thus resolve the debates related to the petrogenetic and tectonic evolution of this region. Compared with traditional bulk analytical methods, in situ oxygen isotope analysis using a secondary ion mass spectrometer (SIMS) reveals inter- and intra-mineral isotopic variations. This paper presents heterogeneous oxygen isotope data on Ol and orthopyroxenes (Opx) from the Songshugou peridotites. We discuss the origins of high-$\delta^{18}O$ and low-$\delta^{18}O$ minerals in the Songshugou peridotites and provide new insights into the evolution of orogen peridotites.

2. Geological setting and sample descriptions

The Qinling orogenic belt in central China was formed through the collision of the North China Block (NCB) and the South China Block (SCB; Fig. 1a) and preserves the evidence of multiple tectonothermal events (Meng and Zhang 2000). The Qinling orogenic belt is composed of four tectonic units from north to south: 1) the southern margin of the

NCB, 2) the North Qinling Belt (NQB), 3) the South Qinling Belt (SQB), and 4) the northern margin of the SCB, separated by the Luonan-Luanchuan-Fangcheng fault (LLFF), Shangnan-Danfeng suture zone (SDSZ), and Mianlue suture zone (MLSZ) (Fig. 1b). Neoproterozoic ophiolite mélanges occur along the SDSZ and indicate of the past existence of an ancient ocean (Dong et al. 2008). The Songshugou peridotites are exposed to the north of SDSZ and are geographically located in the Shanxi and Henan provinces of China. The Songshugou peridotites occur within amphibolite of the Qinling Group as several hundred blocks. The largest massif is about 18 km long and up to 2 km wide, and covers an area of ~20 km^2, forming a NW-SE trending block (Fig. 1c). The amphibolites enclosed the peridotite as lenses in the field which are separated from the Qinling Group by Jieling ductile shear zone in the north and Xigou fault in the south (Fig 1c). Some studies have confirmed that the protoliths of these amphibolites were oceanic basalts (Dong et al., 2008). Some garnet amphibolite dykes occur as discontinuous lenses around Songshugou peridotites. These amphibolites were formed in the Neoproterozoic and underwent peak metamorphism at ~490 Ma, followed by retrograde metamorphism at 460 Ma (Yu et al., 2016). Thus, in one of the popular models the Songshugou peridotites represent fragments of the Neoproterozoic fossil oceanic lithospheric mantle (Dong et al., 2008; Wang et al., 2005; Yu et al., 2016; Zhang et al., 2015) and which experienced subduction and subsequent exhumation along with the overlying amphibolite in the Paleozoic (Yu et al., 2016, 2017; Zhang et al., 2015).

The Songshugou peridotites are dominantly dunites (85 vol% of the Songshugou mylonitized peridotites) with subordinate harzburgite. Dunite can be divided into three groups: coarse-grained dunite (Ol mostly>4 mm; Fig. 2a, b), medium-grained dunite (Ol mostly from 1-4 mm; Fig. 2c, d), and fine-grained dunite (Ol mostly <1 mm; Fig. 2e). Medium to coarse-grained dunite constitute about 15 vol% of the peridotites and occur mainly as variously sized lenses wrapped within the fine-grained dunites. The dunites are unweathered (LOI: 0.56-4.65%; Yu et al. 2017) and are composed dominantly of Ol (90-96 vol%) and chromite (Chr: 1-7 vol%), with variable amphibole (Amp: 1-7 vol%), serpentine (Srp), chlorite (Chl) and talc. The large elongated Ol grains (≥4 mm; 50–70 vol%) in the coarse-grained dunites have preferred orientation and deformation lamellae. The medium- and fine-grained dunites have porphyroclastic and mylonitic texture as a result of mylonitization of varying intensities. Fine-grained dunite is the main rock type in the Songshugou peridotite. The residual medium-grained Ol grains after stretching and fragmentation are preserved in the fine-grained dunites as porphyroclasts (Fig. 2c). Harzburgite forms lenses of various sizes in the peridotites. The major minerals in harzburgite are Ol (64-73 vol%), Opx (22-28 vol%), Amp (1-7 vol%), and minor Chr (1-3 vol%). The large Opx (2-5 mm) grains show preferred orientation and deformation (Fig. 2f). Detailed petrographic descriptions have been reported in Yu et al. (2017).

3. Analytical methods

Major elements in Ol and Opx were measured using a JEOL JXA-8100 Electron Probe MicroAnalyzer (EPMA) with an accelerating potential of 15 kV, sample current of 10 nA with 4 μm diameter beam and 10-30 s counting time on peak at the Institute of Geology and Geophysics (IGG), Chinese Academy of Sciences. The precisions of all analyzed elements are better than 1.5%. Natural and synthetic minerals were used for standard calibration, and a program based on the ZAF procedure was used for matrix corrections. The uncertainty of Fo in Ol is negligible because of high MgO and FeO contents.

Oxygen isotope compositions of Ol were analyzed in situ using a CAMECA IMS-1280 ion microprobe at IGG, including 20 grains in 5 coarse-grained dunites, 26 grains in 7 medium-grained dunites, 13 grains in 4 fine-grained dunites and 9 grains in 3 harzburgites. Sample chips were prepared in epoxy adjacent to grains of a San Carlos Ol intra-laboratory standard and then polished to a flat, smooth surface. The Cs^+ primary beam was accelerated at 10 kV with an intensity of ~2 nA. The spot size was about 20 μm in diameter (10 μm beam diameter plus 10 μm raster). An electron gun was used to compensate for sample charging during analysis. Secondary ions were extracted with a ~10 kV potential. Oxygen isotopes were measured in multi-collector mode with two off-axis Faraday cups. The instrumental mass fractionation factor is corrected using San Carlos Ol standard ($\delta^{18}O$=5.25%; Eiler et al. 1995). The matrix effect was negligible for Ol in the Songshugou peridotites because these Ol have high Fo values, ranging from 90.9-92.9 (Isa et al., 2017; Tang et al., 2019). External reproducibility of Ol standards was typically better than 0.4‰ (2σ). Detailed analytical procedures have been reported in Kita et al. (2009), Tang et al. (2015) and Peng et al. (2016). Selected crystals of Ol were analyzed across profile lines in order to assess compositional and oxygen isotopic variation. The SIMS spots were

DOI: https://doi.org/10.2138/am-2022-7990. http://www.minsocam.org/

reanalyzed by electron microprobe for chemical compositions. Representative compositions and oxygen isotope data of Ol from the Songshugou dunites are given in Table 1.

The Opx separates from 3 harzburgites were handpicked under a binocular microscope and cleaned in an ultrasonic bath in deionized water for 15 min. Oxygen isotope ratios ($\delta^{18}O$) of Opx were determined using a Finnigan MAT-252 mass spectrometer at the IGG. Samples were reacted overnight with BrF_5 at 500 ºC and oxygen was reacted with hot graphite to yield the CO_2 that was measured. Analytical precision was 0.2-0.3‰.

4. Results

4.1 Major element compositions

The major element and oxygen isotope compositions of Ol in the Songshugou peridotites are given in Table 1. Olivines in the coarse-grained dunites and medium-grained dunites have Fo ranging from 91.5 to 92.9 and from 91.0 to 92.9, respectively. Olivine in the fine-grained dunites has lower Fo contents (90.9 to 91.5) than in the coarse-grained dunites (Fig. 3a, b); Fo values of Ol from the medium-grained dunites span the range of the other two groups. The Fo of Ol in the harzburgites varies from 91.5-92.4.

The NiO contents of Ol in the coarse-grained dunites (0.31-0.44 wt.%) is similar to that of Ol in the harzburgite (0.35-0.44 wt.%, Fig. 3a). The NiO contents of Ol from the medium- and fine-grained dunites overlap completely (0.26-0.41 wt.% and 0.25-0.39 wt.%, respectively), with slightly lower average values than the coarse-grained dunites (Fig. 3a). There is not much difference in MnO content of Ol between dunites and harzburgites, ranging from 0.08-0.17 wt.% (Fig. 3b). The CaO and Al_2O_3 contents of Ol in the dunites and harzburgites are <0.03 wt.% (Table 1).

4.2 Oxygen isotopic compositions

Olivines from all 3 types of dunites have large variations in $\delta^{18}O$ values (4.03 to 7.07‰; Table 1). Although some olivines in the dunite have typical mantle $\delta^{18}O$ values (5.7±0.2‰; Mattey et al. 1994; Harmon and Hoefs 1995; Eiler et al. 1997), the majority are either lower or higher than typical mantle $\delta^{18}O$ values (Fig. 4a-c). Different sized Ol crystals in the dunites have distinct $\delta^{18}O$ values. Generally, Ol with smaller grain sizes tend to have higher $\delta^{18}O$ values than the large Ol. Olivines from coarse-grained dunites have $\delta^{18}O$ values ranging from 4.03 to 6.41‰ (Fig. 4a). The Ol from medium- and fine-grained dunites have $\delta^{18}O$ values of 4.44-7.03‰ and 4.32-7.07‰, respectively (Fig. 4b, c).

The $\delta^{18}O$ values of some dunite Ol crystals vary from core to rim (Fig. 5a). The cores of Ol porphyroclasts usually have relatively low $\delta^{18}O$ values, and the rims of Ol porphyroclasts usually have relatively high $\delta^{18}O$ values (Table 1). These Ol appear in the left upper quadrant of the 1:1 lines in $\delta^{18}O$ core vs $\delta^{18}O$ rim plot (Fig. 5b). The lowest $\delta^{18}O$ value of 4.03‰ occurs in the core of an Ol crystal in the coarse-grained dunite (Grain 13 in DSSG13-40; Fig. 4a). However, some cores and rims of medium- and fine-grained Ol have similar but higher $\delta^{18}O$ values than typical mantle (Fig. 4). Individual medium- and fine- grained Ol also have nearly identical $\delta^{18}O$ values between cores and rims within the error (Fig. 5b). The $\delta^{18}O$ values generally increase from cores to rims accompanied by a general decrease in Fo values in some large Ol grains in the dunites (Fig. 6a-d). In addition,

This is the peer-reviewed, final accepted version for American Mineralogist, published by the Mineralogical Society of America.
The published version is subject to change. Cite as Authors (Year) Title. American Mineralogist, in press.
DOI: https://doi.org/10.2138/am-2022-7990. http://www.minsocam.org/

the Songshugou peridotites in the Qinling orogen have both lower and higher $\delta^{18}O$ values than the typical mantle, which is distinct from peridotites in Sulu-Dabie orogen which have lower $\delta^{18}O$ values than the typical mantle (Fig. 7a).

The variation in $\delta^{18}O$ of Ol from harzburgites is smaller than that seen among the grains from dunites. The harzburgite $\delta^{18}O$ values (4.21 to 5.45‰) are equal to or slightly lower than those of typical mantle (Fig. 4d). Opx in three harzburgites have typical mantle $\delta^{18}O$ value (5.5‰, 5.6‰ and 5.8‰, Figs. 4d). Contrary to the core-rim variations for Ol in the dunites, rims of Ol in the harzburgites have lower $\delta^{18}O$ values than those of cores (Fig. 5a, b).

5. Discussion

5.1 Origin of low-$\delta^{18}O$ olivine in the Songshugou peridotites

Many low-$\delta^{18}O$ magmas (Bacon et al. 1989; Balsley and Gregory 1998; Thirlwall et al. 2006; Torch et al. 2020; Kim et al. 2021), igneous rocks (Taylor and Sheppard 1986; Bindeman et al. 2008a, b; Guo et al. 2013; Radu et al. 2019) and metamorphic rocks (Baker and Matthews, 1995; Yui et al. 1995; Baker et al. 1997; Dobosi et al. 2003; Zheng et al. 2003) throughout the world have been reported. Origins of these low-$\delta^{18}O$ rocks generally relate to interaction with meteoric fluids. It is difficult to identify the origin of Ol in the orogenic peridotites, given the range of processes that can produce such oxygen isotope compositions. The low $\delta^{18}O$ values of Songshugou peridotites always occur in the cores of large Ol porphyroclasts. This suggests that low-$\delta^{18}O$ Ol formed prior to mylonitization.

Therefore, the protoliths of these peridotites were depleted in ^{18}O before subduction. One possibility is that high-temperature water-rock interactions in the peridotites result in low $\delta^{18}O$ values of Ol (Rouméjon et al. 2018; Zakharov et al. 2019; Kim et al. 2021). Meteoric-hydrothermal alteration and seawater-hydrothermal alteration are two candidates for the ^{18}O-depleted fluids (Fig. 7c) that led to generation of low-$\delta^{18}O$ Ol (as low as 4.03‰) in Songshugou peridotites. Modern meteoric water in eastern China and seawater have $\delta^{18}O$ values of -8 to -6‰ and ~0‰, respectively which contains light oxygen relative to SMOW (Balsley and Gregory 1998; Zheng et al. 1998; Alt and Bach 2006; Pack and Herwartz 2014; Hodel et al. 2018). Previous studies have demonstrated that the Songshugou peridotites represent fragments of the fossil oceanic lithospheric mantle that experienced subduction in the Early Paleozoic (Yu et al. 2016, 2017). This rules out the possibility of meteoric water infiltration into the Songshugou peridotites through the overlying rocks prior to subduction, and therefore seawater-peridotite interaction is a more plausible explanation. Oxygen isotope studies on the Samail ophiolite, Sultanate of Oman, indicate that pervasive subsolidus hydrothermal exchange with seawater occurred throughout the upper 75% of an 8 km thick oceanic crustal section, and that seawater even penetrated down into the peridotites (Gregory and Taylor 1981). Similarly, low-$\delta^{18}O$ seawater could infiltrate into the Songshugou peridotites along faults or fractures, resulting in the formation of low-$\delta^{18}O$ Ol.

Olivines in all harzburgites have lower $\delta^{18}O$ values than the normal mantle values, whereas the Opx in the harzburgite have typical mantle $\delta^{18}O$ values, reflecting different exchange rates for Ol and Opx with the seawater. Orthopyroxene exchanges oxygen much more slowly with external fluid than does Ol or Spinel (Gregory and Taylor 1986a, b). Thus, Ol could have acquired low $\delta^{18}O$ more efficiently than coexisting Opx by interaction with ^{18}O-depleted fluids in the oceanic lithospheric mantle. Songshugou peridotites were affected by the infiltration of external fluids during exhumation which are related to the metasomatic enrichments in large ion lithophile elements (LILE) and the crystallization of amphibole. Amphiboles are common in the Songshugou peridotites. During the exchange between metasomatic fluids and the mineral assemblage, oxygen isotopic compositions of amphiboles were significantly affected. In addition, the average grain size of Ol and Opx in harzburgites is larger than that the dunite. Thus, Ol and Opx in the harzburgites have probably preserved low $\delta^{18}O$ values and typical mantle $\delta^{18}O$ values to the greatest degree during exhumation.

Songshugou peridotites could reside at mantle depths during subduction for a short time, otherwise the low $\delta^{18}O$ signature in Ol would not be preserved. This process is similar to the evolution of ultra-high pressure (UHP) metamorphic mafic and ultramafic rocks with low-$\delta^{18}O$ Ol in Sulu-Dabie orogen, eastern China (Fig 7a; Yui et al. 1995; Zheng et al. 1998; Zhang et al. 2000; Zheng et al. 2003). Eclogites and Ol in peridotites in the Sulu-Dabie orogen acquired the relatively low $\delta^{18}O$ values (-10 to -9‰ and 2.9 to 3.8‰, respectively) by interaction with meteoric water prior to eclogite-facies metamorphism during subduction but also precludes the infiltration of external fluids during exhumation because of relatively rapid cooling and ascent. The maximum time scale for the oxygen isotopic reequilibration of Sulu-Dabie eclogites residence at mantle depths would probably be less than ~20 Ma, assuming an eclogite slab of 10–20 km thickness (Zheng et al. 1998). Songshugou peridotites experienced subduction along with the amphibolites. The geochronological studies show that the HP/UHP metamorphic rocks of the Qinling group underwent eclogite-facies prograde metamorphism at 480–500 Ma (Liu et al. 2013; Zhang et al. 2015 and their references therein). This is compatible with the timing of peak metamorphism of Songshugou amphibolites (501-483 Ma) determined by Yu et al (2016). Thus, the duration these peridotites resided at mantle depths would probably be < 18-20 Ma. A number of studies have addressed the preservation of pre-metamorphic isotopic compositions through high-grade metamorphism during subduction (Baker and Matthews 1995; Yui et al. 1995; Matthews et al. 1996; Baker et al. 1997; Zheng et al. 1998). The high-$\delta^{18}O$ melt/fluid derived from subducted continental materials only increased the $\delta^{18}O$ values in the large Ol rims and some medium- and fine-grained Ol in the dunites, but could not alter the low $\delta^{18}O$ values in the cores of Ol porphyroclasts.

5.2 High-δ^{18}O signature of olivine

The high-$\delta^{18}O$ signatures found in Ol porphyroclast rims and some fine grained Ol from the Songshugou dunites could be produced by interaction with melts/fluids during recrystallization. Studies on ophiolites have demonstrated that the upper oceanic crustal materials that experienced low-temperature alteration have a high-$\delta^{18}O$ signature (Gregory and Taylor 1981; Eiler et al. 1995; Putlitz et al. 2000; Hansteen and Troll 2003). It has been proposed that slab dehydration during subduction process can produce the high $\delta^{18}O$ signature in altered upper ocean crust from ophiolites, because the $\delta^{18}O$-enriched melts/fluids necessary to impart that signature could be derived from the subducted oceanic or continental crustal materials (Bebout et al. 1989; Barnicoat and Cartwright 1995, 1997; Putlitz et al. 2000; Underwood and Clynne 2017; Heinonen et al. 2018). The high-$\delta^{18}O$ feature of Ol in the Songshugou dunites requires addition of $\delta^{18}O$-enriched component. Previous studies on the Songshugou peridotites have revealed that these rocks had experienced melt/fluid additions during mylonitization in the process of subduction and exhumation (Yu et al. 2017). This process has resulted in a decrease in Fo values and grain sizes of Ol in the dunites. Systematic variations of chemical composition zoning and $\delta^{18}O$ values could be observed in the Ol if melt/fluid interacts with the Ol. Accordingly, the rims of Ol porphyroclasts usually have higher $\delta^{18}O$ values than that in the cores (Fig. 5a, b). Furthermore, $\delta^{18}O$ and Fo values in the Ol porphyroclasts are negatively correlated, such that $\delta^{18}O$ increase and Fo decrease progressively from cores to rims (Fig. 6a-d). Some Ol cores and rims have similar $\delta^{18}O$ values but are all higher than typical mantle (Fig. 4), indicating that oxygen isotope exchange achieved equilibrium between these Ol and ^{18}O-rich melts/fluids. All the above features suggest that the high $\delta^{18}O$ of Ol in the Songshugou dunites formed during mylonitization in the exhumation process with melt/fluid involvement.

The North Qinling Belt, represented by the Qinling Group and the Songshugou peridotites, amphibolites and gneisses, was subducted to the depth of eclogite facies during the Paleozoic (Zhang et al. 2015). Zircons in these amphibolites, gneisses and dikes acquired very high $\delta^{18}O$ (up to 13.9) during amphibolite facies retrograde metamorphism between 454–470 Ma (Fig. 7b), owing to the addition of fluids derived from the dehydration of altered oceanic basalts and the melt of continental sediments (Yu et al. 2016). Previous studies of the minor and trace element variations in chromite had suggested that the Songshugou dunites experienced amphibolite facies retrograde metamorphism at temperature of 610-680 °C with infiltration of fluid (Yu et al. 2019). The ^{18}O-enriched fluids/melts could be efficiently delivered along fractures and shear zones during extensive deformation of the dunites. Thus, the higher than typical mantle $\delta^{18}O$ values of Ol are due to exchange with strongly $\delta^{18}O$-shifted fluids at low temperature (<610-680 °C) in the exhumation process.

6. Implications

Previous studies of the Ol from mantle xenoliths, basalts, and ultrapotassic volcanic rocks have shown that oxygen isotope compositions are relatively homogeneous (Widom and Farquhar 2003; Wang and Eiler 2008; Guo et al. 2013; Liu et al. 2014). Most reported $\delta^{18}O$ data of Ol are equal to or lower than the typical mantle value, including Ol from orogenic peridotites (Wang et al. 2003; Zhang et al. 2000; Zheng et al. 2003; Yu et al. 2010; Zheng 2012). However, olivines from the Songshugou peridotites in the Qinling orogen have both lower $\delta^{18}O$ values and higher $\delta^{18}O$ values relative to the typical mantle. Our major element and oxygen isotopic compositions of Ol and Opx from different types of peridotites, including the cores and rims of multiple crystals, provide new insights into the evolution of the Songshugou orogenic peridotites. We propose (1) Low-$\delta^{18}O$ Ol in the Songshugou peridotites formed as seawater infiltrated into the peridotites along faults or fractures, and exchanged with Ol under high temperature conditions in the oceanic lithosphere mantle prior to subduction. (2) Songshugou peridotites resided at mantle depths during subduction for only a short time (<20 Ma) so that the low $\delta^{18}O$ signature in Ol was preserved. (3) high-$\delta^{18}O$ Ol reflect exchange with melts/fluids derived from the dehydration of altered oceanic basalts and seafloor sediments during the exhumation process.

In addition to the significant applications to mineralogy and petrology of orogenic peridotites, this study has important implications for understanding the tectonic affinity and evolution of Songshugou peridotites and North Qinling Orogen. The heterogeneous $\delta^{18}O$ data in the Ol and Opx further demonstrates that the Songshugou peridotites represent Neoproterozoic oceanic lithospheric mantle that experienced subduction and exhumation during the Early Paleozoic (Yu et al. 2017). Therefore, this study has improved our understanding of the geodynamic processes of orogenic peridotites and the tectonic evolution of the North Qinling Orogen.

Acknowledgements

The authors would like to thank Yanjie Tang, Benxun Su, Yan Xiao and Juan Zhang for their assistance with sample collection and preparation. We would like to thank YaDong

Liu, Jiao Li, Guoqiang Tang, and LianJun Feng for their assistance in oxygen isotopic analysis. We are grateful to Paul Tomascak, Nicole E. Moore, Xiaoping Xia and an anonymous reviewer for their comments that greatly improved the quality of this manuscript.

Funding

This research was financially supported by the National Key Research and Development Project of China (Grant 2019YFA0708603) and the National Natural Science Foundation of China (Grant 41603037).

References cited

Alt, J.C., and Bach, W. (2006) Oxygen isotope composition of a section of lower oceanic crust, ODP Hole 735B. Geochemistry Geophysics Geosystems, 7, 1–18.

Bacon, C.R., Adami, L.H., Lanphere, M.A. (1989) Direct evidence for the origin of low-^{18}O silicic magmas: quenched samples of a magma chamber's partially-fused granitoid walls, Crater Lake, Oregon. Earth and Planetary Science Letters, 96, 199–208.

Baker, J., and Matthews A. (1995) The stable isotopic evolution of a metamorphic complex, Naxos, Greece. Contribution to Mineralogy Petrollogy, 120, 391–403.

Baker, J., Matthews, A., Mattey, D., Rowley, D., Xue, F. (1997) Fluid-rock interactions during ultra-high-pressure metamorphism, Dabie Shan, China. Geochimical et Cosmochimica Acta, 8, 685–1696.

DOI: https://doi.org/10.2138/am-2022-7990. http://www.minsocam.org/

Balsley, S.D., and Gregory, R.T. (1998) Low-^{18}O silicic magmas: why are they so rare? Earth and Planetary Science Letters, 162, 123–136.

Barnicoat, A.C., and Cartwright, I. (1997) The gabbro-eclogite transformation: an oxygen isotope and petrographic study of west Alpine ophiolites. Journal of metamorphic Geology, 15, 93–104.

Barnicoat, A.C., and Cartwright, I. (1995) Focused fluid flow during subduction: Oxygen isotope data from high-pressure ophiolites of the western Alps. Earth and Planetary Science Letters, 132, 53–61.

Bebout, G.E., and Barton, M.D. (1989) Fluid flow and metasomatism in a subduction zone hydrothermal system: Catalina Schist terrane, California. Geology, 17, 976–980.

Bindeman, I.N., Brooks, C.K., McBirney, A.R. Taylor, H.P. (2008a) The Low-δ18O Late-Stage Ferrodiorite Magmas in the Skaergaard Intrusion: Result of Liquid Immiscibility, Thermal Metamorphism, or Meteoric Water Incorporation into Magma? The Journal of Geology, 116, 571–586.

Bindeman, I.N., Gurenko, A.A., Sigmarsson, O, Chaussidon, M. (2008b) Oxygen isotope heterogeneity and disequilibria of olivine crystals in large volume Holocene basalts from Iceland: Evidence for magmatic digestion and erosion of Pleistocene hyaloclastites. Geochimical et Cosmochimica Acta, 72, 4397–4420.

Cao, Y., Song, S.G., Su, L., Jung, H., Niu, Y.L. (2016). Highly refractory peridotites in Songshugou, Qinling orogen: insights into partial melting and melt/fluid-rock reaction in the forearc mantle. Lithos, 252, 234–254.

Carmody, L., Barry, P.H., Shervais, J.W., Taylor, L.A. (2013) Oxygen isotopes in subducted oceanic crust: A new perspective from Siberian diamondiferous eclogites. Geochemistry, Geophysics, Geosystems, 14, 3479–3493.

Dallai, L., Bianchini, G., Avanzinelli, R., Natali, C., Conticelli, S. (2019) Heavy oxygen recycled into the lithospheric mantle: Scientific Reports, 9, 1–7.

Deines, P., and Haggerty, S.E. (2000). Small-scale oxygen isotope variations and petrochemistry of ultradeep (>300 km) and transition zone xenoliths. Geochimica et Cosmochimica Acta, 64, 117–131.

Dijkstra, A.H., Drury, M.R., Vissers, R.L.M., Newman, J., 2002. On the role of melt-rock reaction in mantle shear zone formation in the Othris Peridotite Massif (Greece). Journal of Structural Geology 24, 1431–1450.

Dobosi, G., Kempton, P.D., Downes, H., Embey-Isztin，A., Thirlwall, M., Greenwood, P. (2003) Lower crustal granulite xenoliths from the Pannonian Basin, Hungary, Part 2: Sr-Nd-Pb-Hf and O isotope evidence for formation of continental lower crust by tectonic emplacement of oceanic crust. Contributions to Mineralogy and Petrology, 144, 671–683.

Dong, Y.P., Zhou, M.F., Zhang, G.W., Zhou, D.W., Liu, L., Zhang, Q. (2008) The Grenvillian Songshugou ophiolite in the Qinling Mountains, Central China: Implications for the tectonic evolution of the Qinling orogenic belt. Journal of Asian Earth Sciences, 32, 325–335.

Eiler, J.M. (2001) Oxygen isotope variations in basaltic lavas and upper mantle rocks.

Reviews in Mineralogy and Geochemistry, 43, 19–364.

Eiler, J.M., Farley, K.A., Valley, J.W., Hauri, E., Craig, H., Hart, S.R., Stolper, E.M. (1997) Oxygen isotope variations in ocean island basalt phenocrysts. Geochimica et Cosmochimica Acta, 61, 2281–2293.

Eiler, J.M., Farley, K.A., Valley, J.W., Stolper, E.M., Hauri, E.H., Craig, H. (1995) Oxygen isotope evidence against bulk recycled sediment in the mantle sources of Pitcairn Island lavas. Nature, 377, 138–141.

Genske, F.S., Beier, C., Haase, K.M., Turner, S.P., Krumm, S., Brandl, P.A. (2013) Oxygen isotopes in the Azores islands: Crustal assimilation recorded in olivine. Geology, 41, 491–494.

Gregory, R.T., and Taylor, H P. (1981) An oxygen isotope profile in a section of Cretaceous oceanic crust, Samail Ophiolite, Oman: Evidence for $\delta^{18}O$ buffering of the oceans by deep (>5 km) seawater-hydrothermal circulation at mid-ocean ridges. Journal of Geophysical Research, 86, 2737–2755.

Gregory, R.T., and Taylor, H.P. (1986a) Non-equilibrium, metasomatic $^{18}O/^{16}O$ effects in upper mantle mineral assemblages. Contribution to Mineralopgy and Petrology, 93, 124–135.

Gregory, R.T., and Taylor, H.P. (1986b) Possible non-equilibrium oxygen isotope effects in mantle nodules, an alternative to the Kyser-O'Neil-Carmichael $^{18}O/^{16}O$ geothermometer. Contributions to Mineralogy and Petrology, 93, 114–119.

Guo, F., Guo, J.T., Wang, Y., Fan, W.M., Li, C.W., Li, H.X., Zhao, L. (2013) A metasomatized mantle wedge origin for low-δ^{18}O olivine in late Cretaceous Junan and Qingdao basalts in the Sulu orogen. Chinese Science Bulletin, 58, 3903–3913.

Hansteen, T.H., Troll, V.R. (2003) Oxygen isotope composition of xenoliths from the oceanic crust and volcanic edifice beneath Gran Canaria (Canary Islands): consequences for crustal contamination of ascending magmas. Chemical Geology 193, 181–193.

Hao, Y.T., Xia, Q.K., Dallai, L, Coltorti, M. (2015) Recycled oceanic crust-derived fluids in the lithospheric mantle of eastern China: Constraints from oxygen isotope compositions of peridotite xenoliths. Lithos, 228–229, 55–61.

Harmon, R.S., and Hoefs, J. (1995) Oxygen isotope heterogeneity of the mantle deduced from global ^{18}O systematics of basalts from different geotectonic settings. Contribution to Mineralogy and Petrollogy, 120, 95–114.

Heinonen, J.S., Luttinen, A.V., Whitehouse, M.J. (2018) Enrichment of 18O in the mantle sources of the Antarctic portion of the Karoo large igneous province[J]. Contributions to Mineralogy and Petrology, 173, 21.

Hodel, F., Macouin, M., Trindade, R.I.F., Triantafyllouet, A. et al. (2018) Fossil black smoker yields oxygen isotopic composition of Neoproterozoic seawater. Nature Communications, 9, 1–7.

Hu, J., Jiang, N., Carlson, R.W., et al. (2019) Metasomatism of the crust-mantle boundary by melts derived from subducted sedimentary carbonates and silicates. Geochimica et Cosmochimica Acta, 11304.

Isa, J., Kohl, I.E., Liu M.C., Wasson J.T., Young E.D., McKeegan, K.D. (2017) Quantification of oxygen isotope SIMS matrix effects in olivine samples: Correlation with sputter rate. Chemical Geology, 458, 14–21.

Jakob, J., Boulvais, P., Andersen, T.B. (2018) Oxygen and carbon isotope compositions of carbonates in a prominent lithologically mixed unit in the central South Norwegian Caledonides. International Journal of Earth Sciences: Geologische Rundschau, 107, 1445–1463.

Kim, N.K., Lee, M.J., Lee, J.I., Kim, J. (2021) Oxygen isotope record of magmatic evolution of alkaline volcanic rocks at The Pleiades, northern Victoria Land, Antarctica. Geosciences Journal, 25, 1–11

Kita, N.T., Ushikubo, T., Fu, B., Valley, J.W. (2009) High precision SIMS oxygen isotope analysis and the effect of sample topography. Chemical Geology 264, 43–57.

Liu, C.Z., Wu, F.Y., Chung, S.L., Li, Q.L., Sun, W.D., Ji, W.Q. (2014) A 'hidden' ^{18}O-enriched reservoir in the sub-arc mantle. Scientific Reports, 4, 4232.

Liu, J., Xia, Q.K., Deloule, E., Ingrin, J, Chen, H., Feng, M. (2015) Water Content and Oxygen Isotopic Composition of Alkali Basalts from the Taihang Mountains, China: Recycled Oceanic Components in the Mantle Source. Journal of Petrology, 4, 681–702.

Liu, L., Liao, X.Y., Zhang, C.L., Chen, D.L., Gong, X.K., Kang, L. (2013) Multi-metamorphic timings of HP/UHP rocks in the North Qinling and their geological implications. Acta Petrologica Sinica, 29, 1634–1656.

DOI: https://doi.org/10.2138/am-2022-7990. http://www.minsocam.org/

Marshall, E.W., Barnes, J.D., Lassiter, J.C. (2017) The role of serpentinite-derived fluids in metasomatism of the Colorado Plateau (USA) lithospheric mantle. Geology, 45, 1103–1106.

Mattey, D., Lowry, D., Macpherson, C. (1994) Oxygen isotope composition of mantle peridotite. Earth and Planetary Science Letters, 128, 231–241.

Matthews, A, Liati, A., Mposkos, E., Skarpelis, N. (1996) Oxygen isotope geochemistry of the Rhodope polymetamorphic terrain in northern Greece: evidence for preservation of pre-metamorphic isotopic composition. European Journal of Mineralogy, 8, 1139–1151.

Meng, Q.R., and Zhang, G.W. (2000) Geologic framework and tectonic evolution of the Qinling orogen, central China. Tectonophysics, 323, 183–196.

Michael, B., Vincent, J.M.S., Enrico, B., 2000. Trace and REE content of clinopyroxenes from supra-subduction zone peridotites: implications for melting and enrichment processes in island arcs. Chemical Geology 165, 67–85.

Moore, N.E., Toth, C., Grunder, A.L., Bohrson, W.A., Bindeman, I. (2016) Oxygen isotope composition of plagioclase from the steens basalt, columbia river basalt province, SE Oregon. 112th Annual GSA Cordilleran Section Meeting.

Nie, H, Yang. J., Zhou, G., Liu, C.Z., et al. (2017) Geochemical and Re-Os isotope constraints on the origin and age of the Songshugou peridotite massif in the Qinling orogen, central China. 292-293, 307–309.

Peng, X.T., Guo, Z.X., House, C.H. Chen, S., Ta, K. (2016) SIMS and NanoSIMS analyses of well-preserved microfossils imply oxygen-producing photosynthesis in the Mesoproterozoic anoxic ocean. Chemical Geology 441, 24–34.

Pack, A., Herwartz, D. (2014) The triple oxygen isotope composition of the Earth mantle and understanding $\Delta^{17}O$ variations in terrestrial rocks and minerals[J]. Earth and Planetary Science Letters, 390, 138–145.

Perkins, G.B., Sharp, Z.D., Selverstone, J. (2006) Oxygen isotope evidence for subduction and rift-related mantle metasomatism beneath the Colorado Plateau-Rio Grande rift transition. Contributions to Mineralogy and Petrology, 151, 633–650.

Putlitz, B., Matthews, A., Valley, J.W. (2000) Oxygen and hydrogen isotope study of high pressure metagabbros and metabasalts (Cyclades, Greece): Implications for the subduction of oceanic crust. Contributions to Mineralogy and Petrology, 138, 114–126.

Radu, I.B., Harris, C., Moine, B.N., Costin, G., Cottin, J.Y. (2019) Subduction relics in the subcontinental lithospheric mantle evidence from variation in the δ 18 O value of eclogite xenoliths from the Kaapvaal craton. Contributions to Mineralogy and Petrology, 174, 18–24.

Riches, A., Ickert, R.B., Pearson, D.G., et al. (2016) In situ oxygen-isotope, major-, and trace-element constraints on the metasomatic modification and crustal origin of a diamondiferous eclogite from Roberts Victor, Kaapvaal Craton. Geochimica et Cosmochimica Acta, 174, 345–359.

Rouméjon, S., Williams, M.J., FrühGreen, G.L. (2018) In-situ oxygen isotope analyses in serpentine minerals: Constraints on serpentinization during tectonic exhumation at slow- and ultraslow-spreading ridges. Lithos, 323, 156–178.

Rui, H.C., Jiao, J.G, Xia, M.Z., Yang, J.S., Xia, Z.D. (2019) Origin of Chromitites in the Songshugou Peridotite Massif, Qinling Orogen (Central China): Mineralogical and Geochemical Evidence. Journal of Earth Science 30, 476–493

Sharp, Z.D., Wostbrock, J.A.G., Pack, A. (2018) Mass-dependent triple oxygen isotope variations in terrestrial materials. Geochemical Perspectives Letters, 7, 27–31.

Song, S. (2006) Evolution from oceanic subduction to continental collision: a case study from the Northern Tibetan plateau based on geochemical and geochronological data. Journal of Petrology, 47, 435-455.

Song, S.G., Su, L., Yang, H.Q., Wang, Y.S. (1998) Petrogenesis and emplacement of the Songshugou peridotite in Shangnan, Shanxi. Acta Petrologica Sinica, 14, 212–221.

Stakes, D.S. and Jr, H.P.T. (1992) The Northern Samail Ophiolite: an oxygen isotope, microprobe, and field study. Journal of Geophysical Research, 97B, 7043–7080.

Su, L., Song, S.G., Zhou, D.W. (2005) Petrogenesis of Songshugou dunite body in the Qinling orogenic belt, Central China: constraints from geochemistry and melt inclusions. Science in China Series D: Earth Sciences, 48, 1146–1157.

Sun, S., Dong, Y.P., Sun, Y.L., Cheng, C., Huang, X.X., Liu, X.M. (2019) Re-Os geochronology, O isotopes and mineral geochemistry of the Neoproterozoic Songshugou ultramafic massif in the Qinling Orogenic Belt, China. Gondwana Research 70, 71–87.

Tang, G.Q., Li, X.H., Li, Q.L., Liu, Y., Liang, X.X., Yin, Q.Z. (2015). Deciphering the physical mechanism of the topography effect for oxygen isotope measurements using a Cameca IMS-1280 SIMS. Journal of Analytical Atomic Spectrometry 30, 950–956.

Tang, G.Q., Su, B.X., Li, Q.L., Xia, X.P., Jing, J.J., Feng, L.J., et al. (2019) High-$Mg^{\#}$ Olivine, Clinopyroxene and Orthopyroxene Reference Materials for *In Situ* Oxygen Isotope Determination. Geostandards and Geoanalytical Research, 43, 585–593.

Taylor, H.P., and Sheppard, S.M.F. (1986) Igneous rocks: I. Processes of isotopic fractionation and isotope systematics. Reviews in Mineralogy and Geochemistry, 16, 227–271.

Thirlwall, M.F., Gee, M.A.M., Lowry, D., Mattey, D.P., Murton, B.J., Taylor, R.N. (2006) Low $\delta^{18}O$ in the Icelandic mantle and its origins: Evidence from Reykjanes Ridge and Icelandic lavas. Geochimica et Cosmochimica Acta, 70, 993–1019.

Troch, J., Ellis, B.S., Harris, C., Bachmann, O., Bindeman, I.N. (2020) Low-$\delta^{18}O$ silicic magmas on Earth: A review. Earth-Science Reviews, 208, 103299.

Underwood, S.J., Clynne, M.A. (2017) Oxygen isotope geochemistry of mafic phenocrysts in primitive mafic lavas from the southernmost Cascade Range, California. American Mineralogist, 102, 252–261.

Valley, J.W., Kinny, P.D., Schulze, D.J., Spicuzza, M.J. (1998) Zircon megacrysts from kimberlite: oxygen isotope variability among mantle melts. Contributions to Mineralogy and Petrology, 133, 1–11.

Vroon, P.Z., Lowry, D., Bergen, MJV , Boyce , A.J., Mattey, D.P. (2001) Oxygen isotope systematics of the Banda Arc: low δ18O despite involvement of subducted continental material in magma genesis. Geochimica et Cosmochimica Acta, 65, 589–609.

Wang, X.B., Yang, J.S., Sheng, R.D., Chen, S.Y. (2005) Qinling Songshugou rocks: ultramafic cumulate complex which underwent amphibolite-facies metamorphism. Acta Geologica Sinica, 79, 174–191.

Wang, Z., and Eiler, J.M. (2008) Insights into the origin of low-δ^{18}O basaltic magmas in Hawaii revealed from in situ measurements of oxygen isotope compositions of olivines. Earth and Planetary Science Letters, 269, 376–386.

Wang, Z., Kitchen, N.E., Eiler, J.M. (2003) Oxygen isotope geochemistry of the second HSDP core. Geochemistry Geophysics Geosystems, 4, 1–29.

Widom, E., and Farquhar, J. (2003) Oxygen isotope signatures in olivines from São Miguel (Azores) basalts: implications for crustal and mantle processes. Chemical Geology, 193, 237–255.

Yu, H., Zhang, H.F., Li, X.H., Zhang, J., Santosh, M., Yang, Y.H., Zhou, D.W. (2016) Tectonic evolution of the North Qinling Orogen from subduction to collision and exhumation: Evidence from zircons in metamorphic rocks of the Qinling Group. Gondwana Research, 30, 65–78.

Yu, H., Zhang, H.F., Santosh, M. (2017) Mylonitized peridotites of Songshugou in the Qinling orogen, central China: A fragment of fossil oceanic lithosphere mantle. Gondwana Research, 52, 1–17.

Yu, H., Zhang, H.F., Zou, H.B., Yang, Y.H. (2019) Minor and trace element variations in chromite from the Songshugou dunites, North Qinling Orogen: Evidence for amphibolite-facies metamorphism. Lithos, 328-329, 146–158.

Yu, S.Y., Xu, Y.G., Ma, J.L., Zheng, Y.F., Kuang, Y.S., Hong, L.B., Ge, W.C., Tong, L.X. (2010) Remnants of oceanic lower crust in the subcontinental lithospheric mantle: Trace element and Sr-Nd-O isotope evidence from aluminous garnet pyroxenite xenoliths from Jiaohe, Northeast China. Earth and Planetary Science Letters, 297, 413–422.

Yui, T.F., Rumble, D.III., Lo, C.H., Li, S.H. (1995) Unusually low $\delta^{18}O$ ultra-high-pressure metamorphic rocks from the Sulu Terrain, eastern China. Geochimica et Cosmochimica Acta, 59, 2859–2864.

Zakharov, D.O., Bindeman, I.N. (2019) Triple oxygen and hydrogen isotopic study of hydrothermally altered rocks from the 2.43-2.41Ga Vetreny belt, Russia: An insight into the early Paleoproterozoic seawater. Geochimica et Cosmochimica Acta, 248, 185–209.

Zakharov, D.O., Bindeman, I.N., Serebryakov, N.S., Prave，A.R., Babarina, I.I. (2019) Low $\delta^{18}O$ rocks in the Belomorian belt, NW Russia, and Scourie dikes, NW Scotland: A record of ancient meteoric water captured by the early Paleoproterozoic global mafic magmatism. Precambrian Research, 33, 105431.

Zhang, H.F., Mattey, D.P., Grassineau, N., Lowry, D., Brownless, M., Gurney, J.J., Menzies, M.A. (2000) Recent fluid processes in the kaapvaal Craton, South Africa: coupled oxygen isotope and trace element disequilibrium in polymict peridotites. Earth and Planetary Science Letters, 176, 57–72.

Zhang, H.F., Yu, H., Zhou, D.W., Zhang, J., Dong, Y.P., Zhang, G.W. (2015) The meta-gabbroic complex of Fushui in north Qinling orogen: A case of syn-subduction mafic magmatism. Gondwana Research, 28, 262–275.

Zhang, R.Y., Liou, J.G., Yang, J.S., Yui, T.F. (2000) Petrochemical constraints for dual origin of garnet peridotites from the Dabie-Sulu UHP terrane, eastern-central China. Journal of Metamorphic Geology, 18, 149–166.

Zhang, R.Y., Rumble, D., Liou, J.G., Wang, Q.C. (1998). Low $\delta^{18}O$, ultrahigh-P garnet-bearing mafic and ultramafic rocks from Dabie Shan, China. Chemical Geology, 150, 161–170.

Zheng Y F. (2012) Metamorphic chemical geodynamics in continental subduction zones. Chemical Geology, 328, 5–48.

Zheng, Y.F., Fu, B., Li, Y.L., Xiao, Y.L., Li, S.G. (1998) Oxygen and hydrogen isotope geochemistry of ultrahigh-pressure eclogites from the Dabie Mountains and the Sulu terrane. Earth and Planetary Science Letters, 155, 113–129.

Zheng, Y.F., Fu, B., Gong, B., Li, L. (2003) Stable isotope geochemistry of ultrahigh pressure metamorphic rocks from the Dabie-Sulu orogen in China: implications for geodynamics and fluid regime. Earth Science Reviews, 62, 105–161.

Zou, H.B., Ma, M.J., Fan, Q.C., Xu, B., Li, S.Q., Zhao, Y.W., King, D.T. (2017) Genesis and open-system evolution of Quaternary magmas beneath southeastern margin of

Tibet: Constraints from Sr-Nd-Pb-Hf isotope systematics. Lithos, 272, 278–290.

This is the peer-reviewed, final accepted version for American Mineralogist, published by the Mineralogical Society of America.
The published version is subject to change. Cite as Authors (Year) Title. American Mineralogist, in press.
DOI: https://doi.org/10.2138/am-2022-7990. http://www.minsocam.org/

Figure Captions

Figure 1 Simplified geological map showing the Songshugou peridotites and sampling locations (modified after Dong et al. 2008). SDSZ: Shangnan-Danfeng suture zone; LLFF: Luonan-Luanchuan-Fangcheng fault; MLSZ: Mianlue suture zone.

Figure 2 Polarized light photomicrographs of the Songshugou peridotites showing placement of analytical spots (circles with x) in individual Ol grains. Data from the analytical traverses is shown in Figure 6. (a, b) Coarse-grained dunites; (d) medium-grained dunite; (c, e) fine-grained dunites; (f) harzburgite.

Figure 3 Plots of (a) NiO and (b) MnO versus forsterite (Fo) contents of olivines in peridotites. CGD: Coarse-grained dunite; MGD: medium-grained dunite; FGD: fine-grained dunite; Harz: harzburgite.

Figure 4 Histograms of $\delta^{18}O$ values in Ol and Opx from Songshugou peridotites. The shaded band respresents $\delta^{18}O$ values of the normal mantle ($\delta^{18}O$=5.7±0.2‰; Mattey et al. 1994; Harmon and Hoefs 1995; Eiler et al. 1997). Core, midpoint and rim are marked by three upper case letters (C, M and R) in the different colored boxes.

Figure 5 Variation of $\delta^{18}O$ values between cores and rims of Ol. (a) Plots of Fo versus $\delta^{18}O$ values of Ol in Songshugou peridotites. Lines connect rim (open) and core (filled) measurements from individual grains. (b) Plots of $\delta^{18}O$ cores versus $\delta^{18}O$ rims of Ol in Songshugou peridotites. Gray shadow represents the $\delta^{18}O$ values of the normal mantle ($\delta^{18}O$=5.7±0.2‰).

Figure 6 The profiles of $\delta^{18}O$ values and Fo contents of individual Ol grains from Fig. 2 (a, b, d, e). The triangles are specifically reporting Fo content for the corresponding circle that reports $\delta^{18}O$ values.

Figure 7 Comparison of $\delta^{18}O$ values in the Songshugou region and other areas. (a) olivine, (b) zircon, and (c) whole rock. Data sources: $\delta^{18}O$ values of Ol in UHP peridotites in Sulu orogen (Zhang et al. 1998; Zheng et al. 2003), MORB and OIB worldwide (Harmon and Hoefs 1995; Eiler et al. 1997); $\delta^{18}O$ values of zircon (Yu et al. 2016); Full range of $\delta^{18}O$ values of whole rock from DSDP are from Eiler (2001) and references therein. The vertical shaded band represents the $\delta^{18}O$ values of upper mantle from Mattey et al. (1994) and Valley et al. (1998). The influence of alteration types on the $\delta^{18}O$ values of Ol are from Gregory and Taylor (1981) and Putlitz et al. (2000).

Table captions

Table 1 Electron microprobe (wt.%) and oxygen isotope (‰) analyses of olivines and orthopyroxenes from Songshugou peridotites.

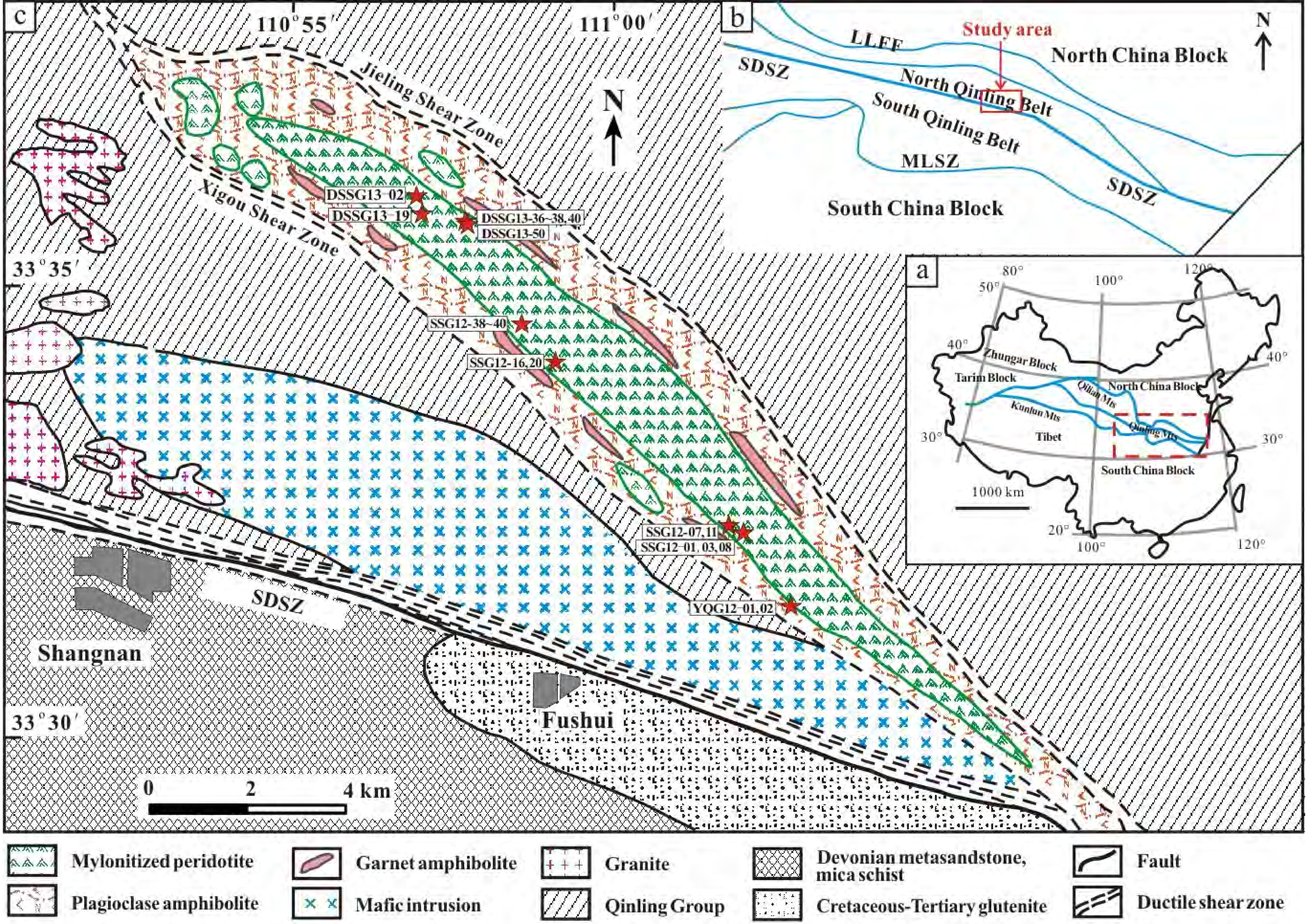
c
110°55′
111°00′
b
LLFF
SDSZ
Study area
North China Block
North Qinling Belt
South Qinling Belt
MLSZ
SDSZ
South China Block
N
Jieling Shear Zone
Xigou Shear Zone
DSSG13-02
DSSG13-19
DSSG13-36~38,40
DSSG13-50
SSG12-38~40
SSG12-16,20
SSG12-07,11
SSG12-01, 03, 08
YQG12-01,02
33°35′
33°30′
SDSZ
Shangnan
Fushui
0
2
4 km
a
80°
100°
120°
50°
40°
40°
30°
30°
20°
100°
120°
Zhungar Block
Tarim Block
North China Block
Qilian Mts
Kunlun Mts
Qinling Mts
Tibet
South China Block
1000 km
Mylonitized peridotite
Plagioclase amphibolite
Garnet amphibolite
Mafic intrusion
Granite
Qinling Group
Devonian metasandstone, mica schist
Cretaceous-Tertiary glutenite
Fault
Ductile shear zone

Figure 1

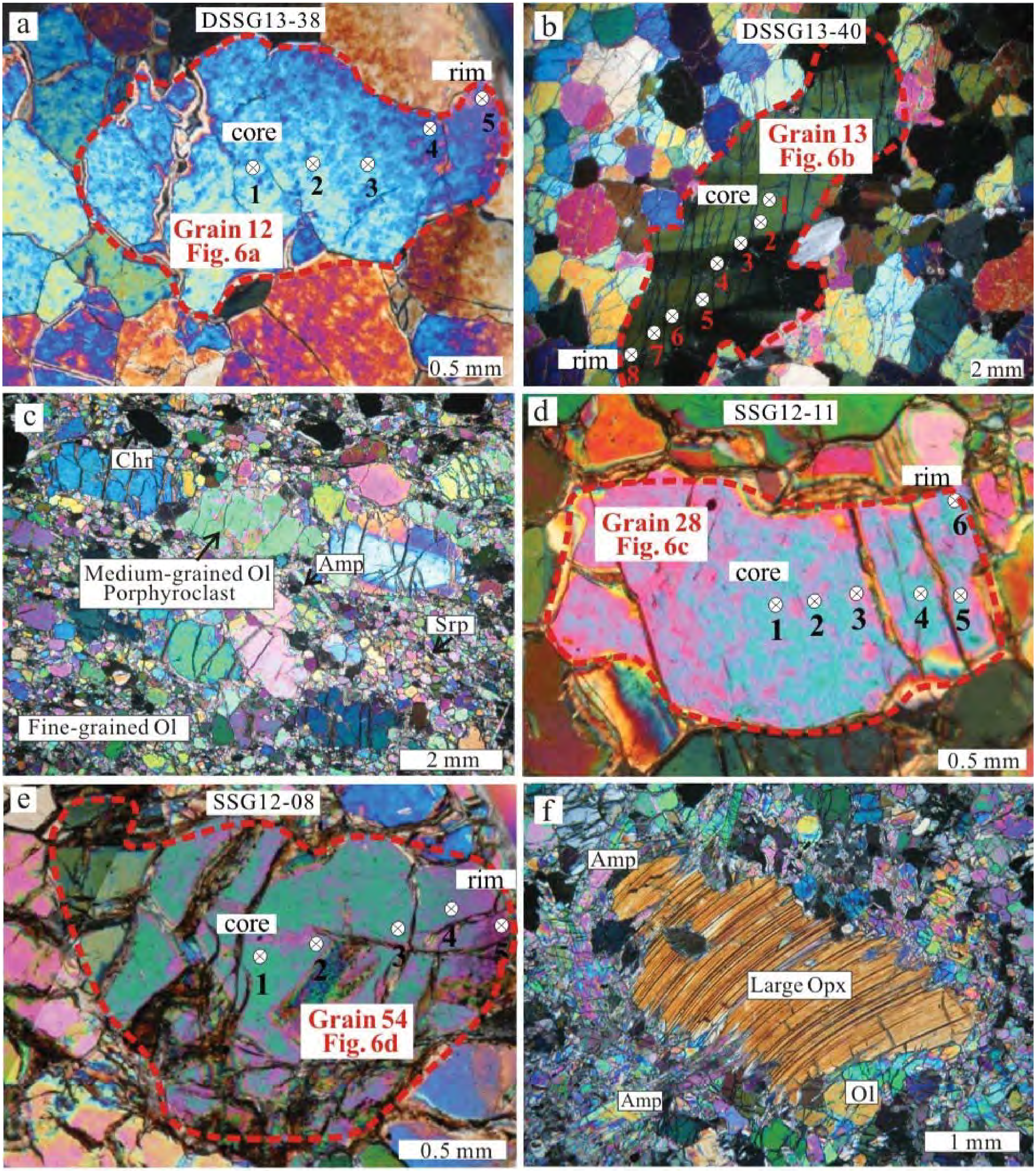

a
DSSG13-38
rim
core
1
2
3
4
5
Grain 12
Fig. 6a
0.5 mm
b
DSSG13-40
Grain 13
Fig. 6b
core
1
2
3
4
5
6
7
8
rim
2 mm
c
Chr
Medium-grained Ol
Porphyroclast
Amp
Srp
Fine-grained Ol
2 mm
d
SSG12-11
rim
Grain 28
Fig. 6c
core
1
2
3
4
5
6
0.5 mm
e
SSG12-08
rim
core
1
2
3
4
5
Grain 54
Fig. 6d
0.5 mm
f
Amp
Large Opx
Amp
Ol
1 mm

Figure 2

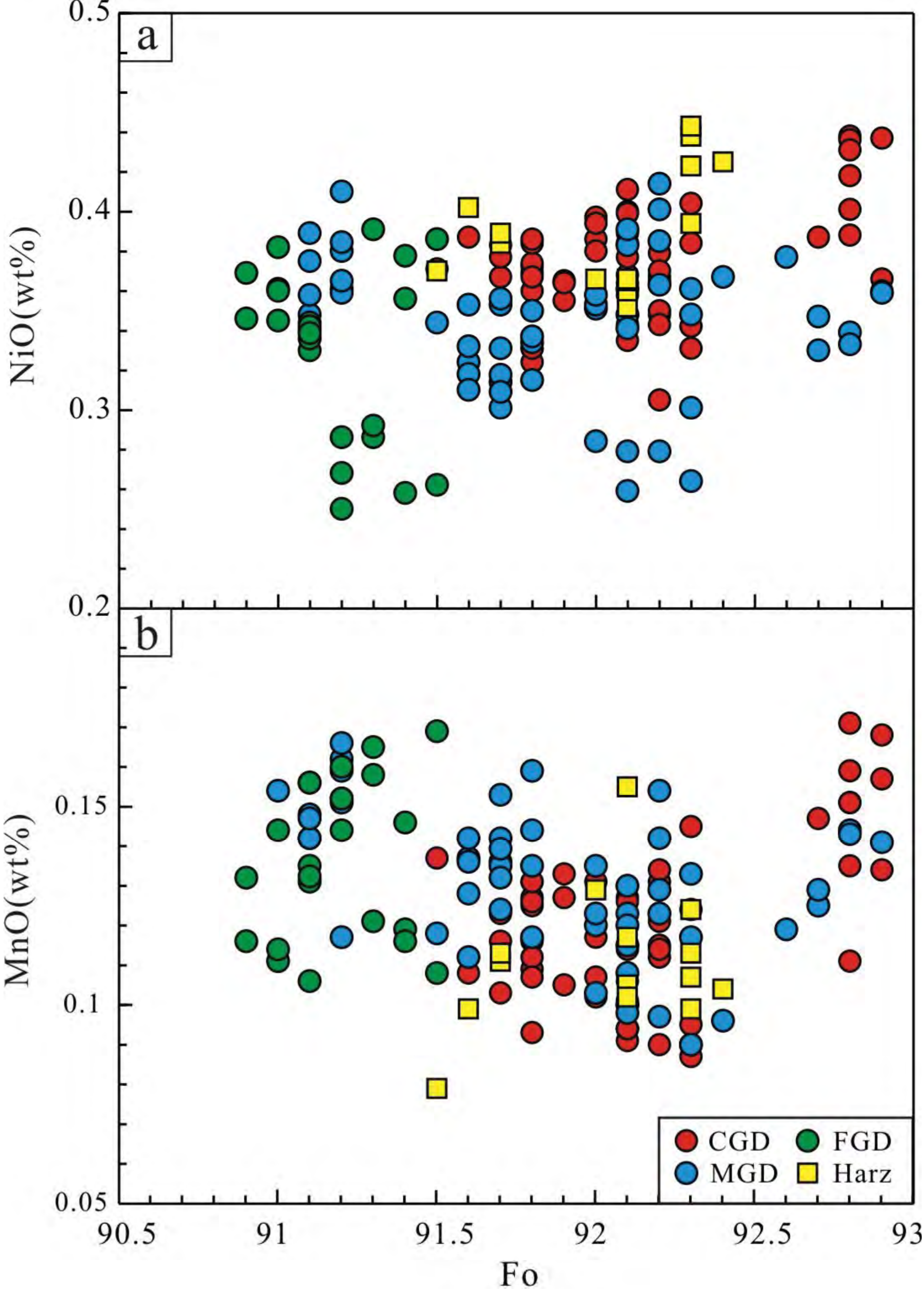
a
b
0.5
0.4
0.3
0.2
0.15
0.1
0.05
NiO(wt%)
MnO(wt%)
90.5
91
91.5
92
92.5
93
Fo
CGD
FGD
MGD
Harz

Figure 3

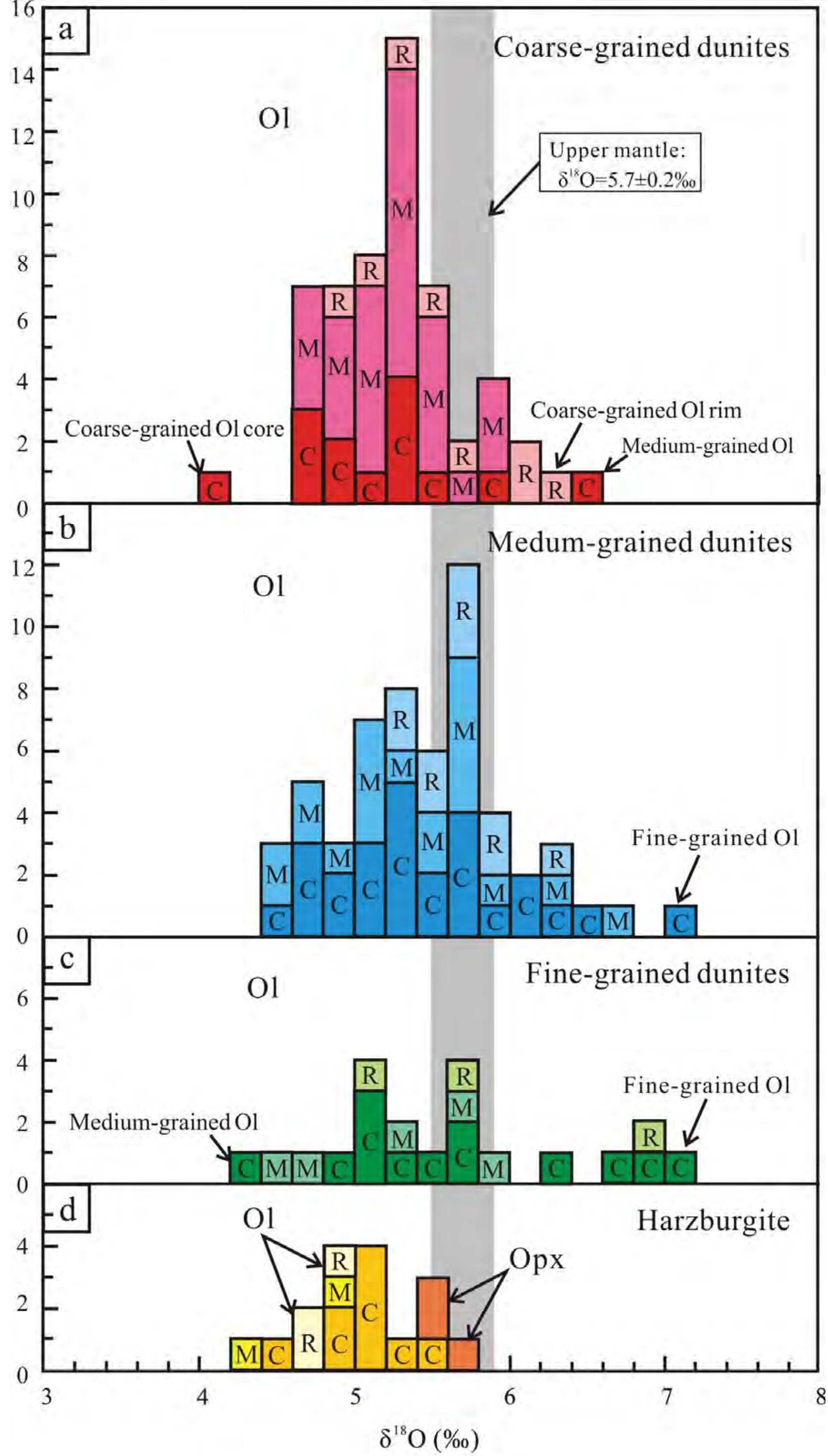

a
Coarse-grained dunites
Ol
Upper mantle:
δ18O=5.7±0.2‰
Coarse-grained Ol core
Coarse-grained Ol rim
Medium-grained Ol
b
Medum-grained dunites
Ol
Fine-grained Ol
c
Fine-grained dunites
Ol
Medium-grained Ol
Fine-grained Ol
d
Harzburgite
Ol
Opx
δ18O (‰)

Figure 4

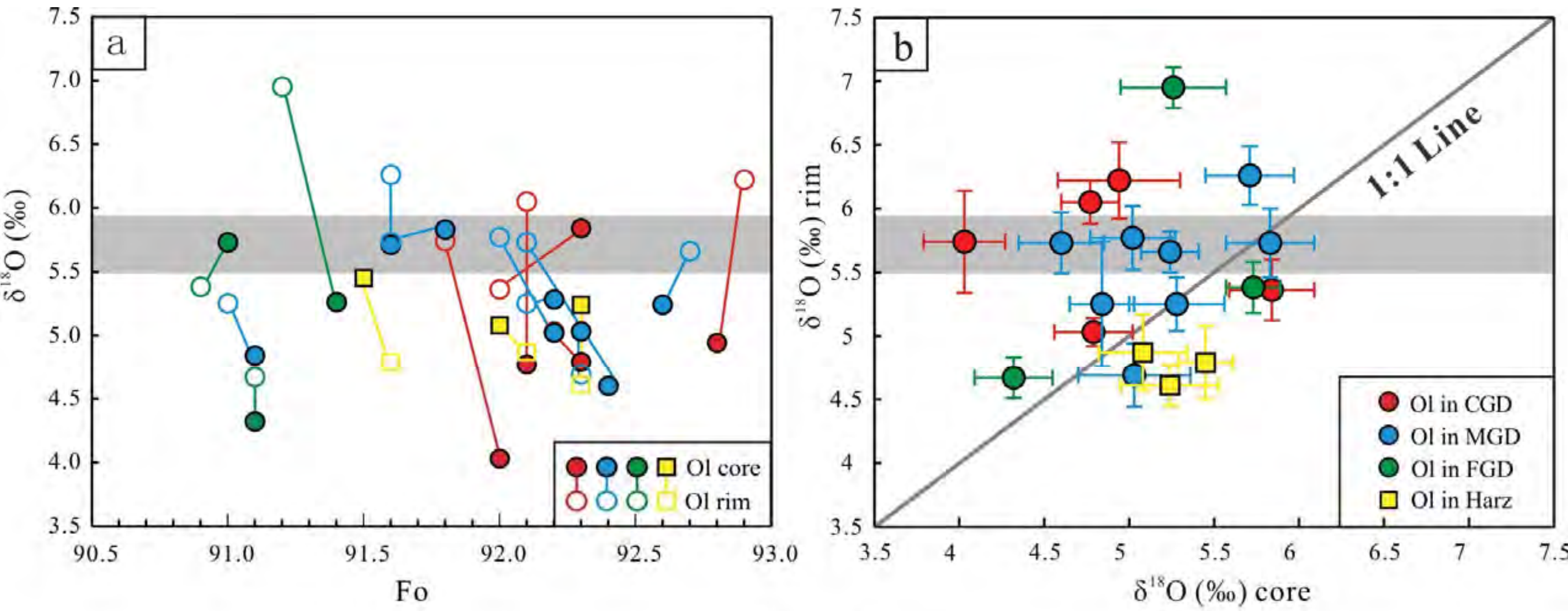

a
b
δ18O (‰)
Fo
Ol core
Ol rim
δ18O (‰) rim
δ18O (‰) core
1:1 Line
Ol in CGD
Ol in MGD
Ol in FGD
Ol in Harz

Figure 5

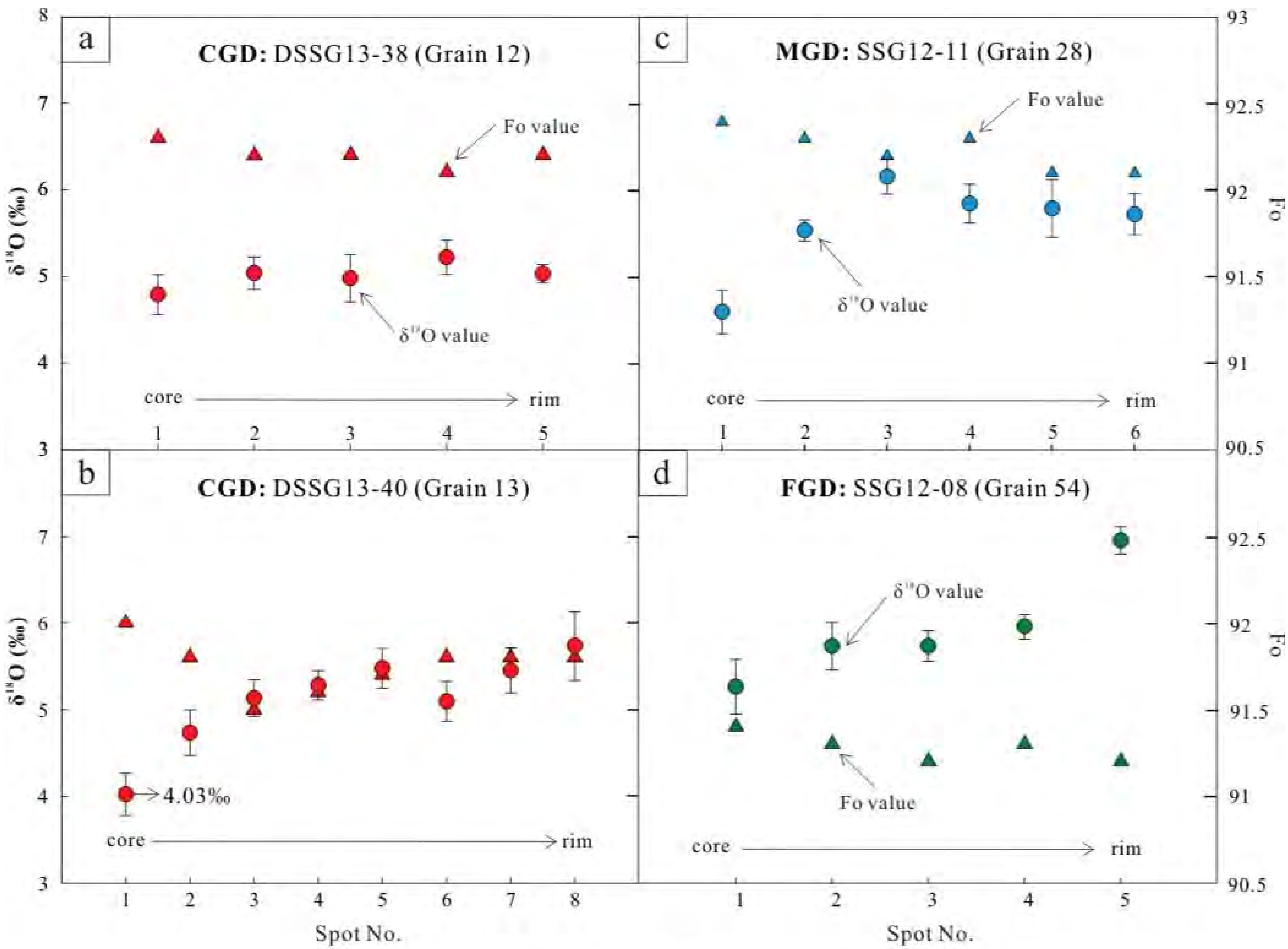

a
CGD: DSSG13-38 (Grain 12)
Fo value
δ18O value
core
rim
b
CGD: DSSG13-40 (Grain 13)
4.03‰
c
MGD: SSG12-11 (Grain 28)
d
FGD: SSG12-08 (Grain 54)
δ18O (‰)
Fo
Spot No.

Figure 6

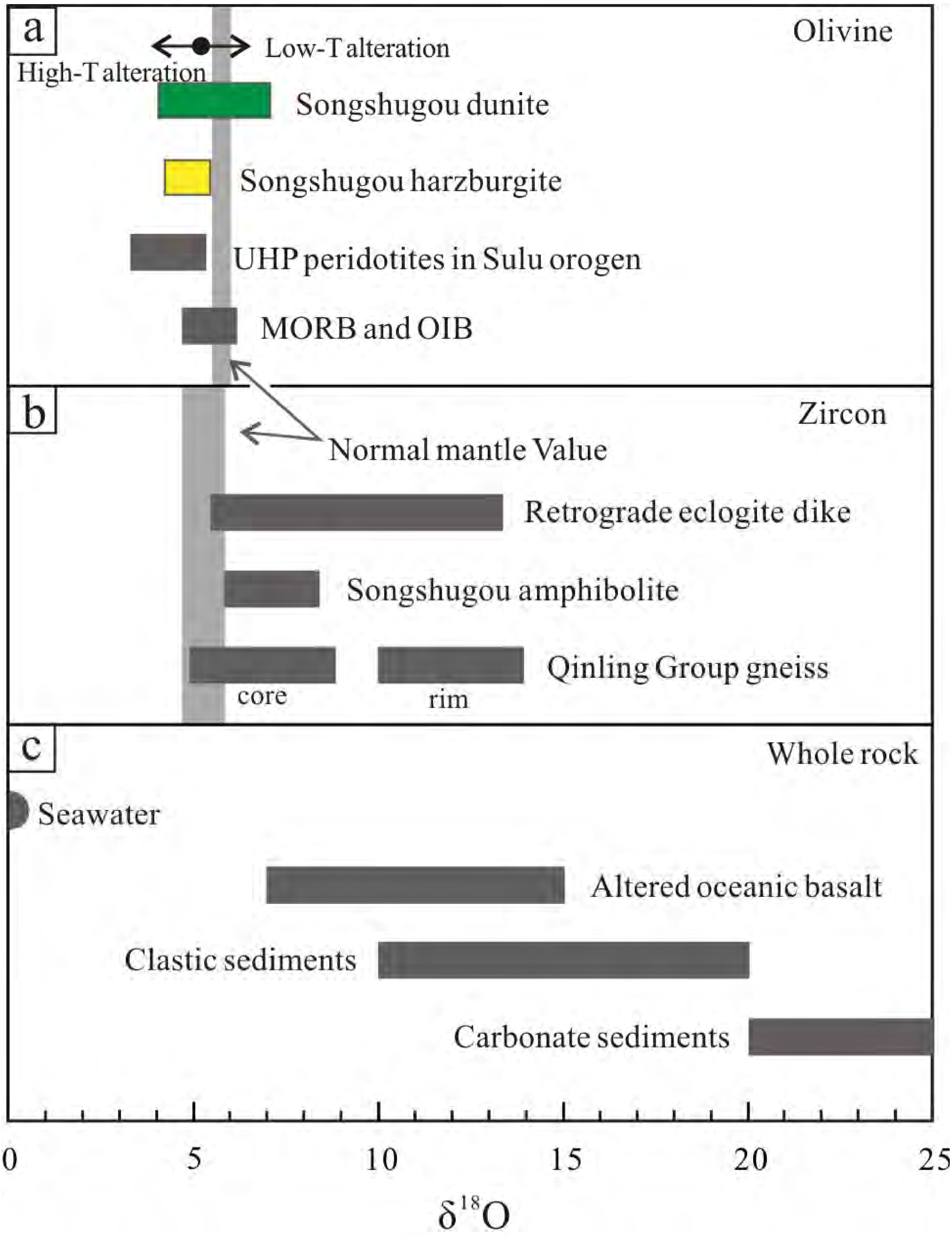
a
Olivine
Low-T alteration
High-T alteration
Songshugou dunite
Songshugou harzburgite
UHP peridotites in Sulu orogen
MORB and OIB
b
Zircon
Normal mantle Value
Retrograde eclogite dike
Songshugou amphibolite
Qinling Group gneiss
core
rim
c
Whole rock
Seawater
Altered oceanic basalt
Clastic sediments
Carbonate sediments
0
5
10
15
20
25
δ18O

Figure 7